

Ps and Qs: Quantization-aware pruning for efficient low latency neural network inference

Benjamin Hawks¹, Javier Duarte², Nicholas J. Fraser³, Alessandro Pappalardo³, Nhan Tran^{1,4}, Yaman Umuroglu³

¹Fermi National Accelerator Laboratory, Batavia, IL 60510, USA

²University of California San Diego, La Jolla, CA 92093, USA

³Xilinx Research, Dublin, D24 T683, Ireland

⁴Northwestern University, Evanston, IL 60208, USA

Correspondence*:

Nhan Tran

ntran@fnal.gov

ABSTRACT

Efficient machine learning implementations optimized for inference in hardware have wide-ranging benefits depending on the application from lower inference latencies to higher data throughputs to more efficient energy consumption. Two popular techniques for reducing computation in neural networks are pruning, removing insignificant synapses, and quantization, reducing the precision of the calculations. In this work, we explore the interplay between pruning and quantization during the training of neural networks for ultra low latency applications targeting high energy physics use cases. However, techniques developed for this study have potential application across many other domains. We study various configurations of pruning during quantization-aware training, which we term *quantization-aware pruning* and the effect of techniques like regularization, batch normalization, and different pruning schemes on multiple computational or neural efficiency metrics. We find that quantization-aware pruning yields more computationally efficient models than either pruning or quantization alone for our task. Further, quantization-aware pruning typically performs similar to or better in terms of computational efficiency compared to standard neural architecture optimization techniques. While the accuracy for the benchmark application may be similar, the information content of the network can vary significantly based on the training configuration.

Keywords: pruning, quantization, neural networks

1 INTRODUCTION

Efficient implementations of machine learning (ML) algorithms provide a number of advantages for data processing both on edge devices and at massive data centers. These include reducing the latency of neural network (NN) inference, increasing the throughput, and reducing power consumption or other hardware resources like memory. During the ML algorithm design stage, the computational burden of NN inference can be reduced by eliminating nonessential calculations through a modified training procedure. In this paper, we study efficient NN design for an ultra-low latency, resource-constrained particle physics application. The classification task is to identify radiation patterns that arise from different elementary particles at

sub-microsecond latency. While our application domain emphasizes low latency, the generic techniques we develop are broadly applicable.

Two popular techniques for efficient ML algorithm design are *quantization* and *pruning*. Quantization is the reduction of the bit precision at which calculations are performed in a NN to reduce the memory and computational complexity. Often, quantization employs fixed-point or integer calculations, as opposed to floating-point ones, to further reduce computations at no loss in performance. Pruning is the removal of unimportant weights, quantified in some way, from the NN. In the most general approach, computations are removed, or pruned, one-by-one from the network, often using their magnitude as a proxy for their importance. This is referred to as magnitude-based unstructured pruning, and in this study, we generically refer to it as pruning. Recently, quantization-aware training (QAT), accounting for the bit precision at training time, has been demonstrated in a number of studies to be very powerful in efficient ML algorithm design. In this paper, we explore the potential of combining pruning with QAT at any possible precision. As one of the first studies examining this relationship, we term the combination of approaches *quantization-aware pruning (QAP)*. The goal is to understand the extent to which pruning and quantization approaches are complementary and can be optimally combined to create even more efficiently designed NNs.

Furthermore, as detailed in Sec. 1.1, there are multiple approaches to efficient NN optimization and thus also to QAP. While different approaches may achieve efficient network implementations with similar classification performance, these trained NNs may differ in their information content and computational complexity, as quantified through a variety of metrics. Thus, some approaches may better achieve other desirable characteristics beyond classification performance such as algorithm robustness or generalizability.

This paper is structured as follows. Section 1.1 briefly recapitulates related work. Section 2 describes the low latency benchmark task in this work related to jet classification at the CERN Large Hadron Collider (LHC). Section 3 introduces our approach to QAP and the various configurations we explore in this work. To study the joint effects of pruning and quantization, we introduce the metrics we use in Section 4. The main results are reported in Section 5. Finally, a summary and outlook are given in Section 6.

1.1 Related work

While NNs offer tremendous accuracy on a variety of tasks, they typically incur a high computational cost. For tasks with stringent latency and throughput requirements, this necessitates a high degree of efficiency in the deployment of the NN. A variety of techniques have been proposed to explore the efficient processing of NNs, including quantization, pruning, low-rank tensor decompositions, lossless compression and efficient layer design. We refer the reader to Ref. [1] for a survey of techniques for efficient processing of NNs, and focus on related work around the key techniques covered in this paper.

Pruning. Early work [2] in NN pruning identified key benefits including better generalization, fewer training examples required, and improved speed of learning the benefits through removing insignificant weights based on second-derivative information. Recently, additional compression work has been developed in light of mobile and other low-power applications, often using magnitude-based pruning [3]. In Ref. [4], the authors propose the *lottery ticket (LT) hypothesis*, which posits that sparse subnetworks exist at initialization which train faster and perform better than the original counterparts. Ref. [5] proposes learning rate rewinding in addition to weight rewinding to more efficiently find the winning lottery tickets. Ref. [6] extends these ideas further to learning “supermasks” that can be applied to an untrained, randomly initialized network to produce a model with performance far better than chance. The current state of pruning is reviewed in Ref. [7], which finds current metrics and benchmarks to be lacking.

Quantization. Reducing the precision of a static, trained network’s operations, *post-training quantization* (PTQ), has been explored extensively in the literature [8, 9, 3, 10–12]. QAT [13–23] has also been suggested with different frameworks like QKERAS [24, 25] and BREVITAS [26, 27] developed specifically to explore quantized NN training. Hessian-aware quantization (HAWQ) [28, 29] is another quantization approach that uses second derivative information to automatically select the relative bit precision of each layer. The Bayesian bits approach attempts to unify structured pruning and quantization by identifying pruning as the 0-bit limit of quantization [30]. In Ref. [31], a combination of a pruning technique and a quantization scheme that reduces the complexity and memory usage of convolutional layers, by replacing the convolutional operation by a low-cost multiplexer, is proposed. In particular, the authors propose an efficient hardware architecture implemented on field-programmable gate array (FPGA) on-chip memory. In Ref. [32], the authors apply different quantization schemes (fixed-point and sum-power-of-two) to different rows of the weight matrix to achieve better utilization of heterogeneous FPGA hardware resources.

Efficiency metrics. Multiple metrics have been proposed to quantify neural network efficiency, often in the context of dedicated hardware implementations. The artificial intelligence quotient (aiQ) is proposed in Ref. [33] as metric to measure the balance between performance and efficiency of NNs. Bit operations (BOPs) [34] is another metric that aims to generalize floating-point operations (FLOPs) to heterogeneously quantized NNs. A hardware-aware complexity metric (HCM) [35] has also been proposed that aims to predict the impact of NN architectural decisions on the final hardware resources. Our work makes use of some of these metrics and further explores the connection and tradeoff between pruning and quantization.

2 BENCHMARK TASK

The LHC is a proton-proton collider that collides bunches of protons at a rate of 40 MHz. To reduce the data rate, an online filter, called the trigger system, is required to identify the most interesting collisions and save them for offline analysis. A crucial task performed on FPGAs in the Level-1 trigger system that can be greatly improved by ML, both in terms of latency and accuracy, is the classification of particles coming from each proton-proton collision. The system constraints require algorithms that have a latency of $\mathcal{O}(\mu\text{s})$ while minimizing the limited FPGA resources available in the system.

We consider a benchmark dataset for this task to demonstrate our proposed model efficiency optimization techniques. In Ref. [36, 8, 37], a dataset [38] was presented for the discrimination of collimated showers of particles, or *jets*, arising from the decay and hadronization of five different classes of particles: light flavor quarks (q), gluons (g), W and Z bosons, and top quarks (t). It consists of jets produced in proton-proton collisions at a center-of-mass energy of 13 TeV, each with a transverse momentum of about 1 TeV. Each jet is represented by 16 physics-motivated high-level features. The dataset contains 870,000 jets, which is split into 472,500 jets for training, 157,500 jets for validation, and 240,000 jets for testing. Adopting the same baseline architecture as in Ref. [8], we consider a fully-connected NN consisting of three hidden layers (64, 32, and 32 nodes, respectively) with rectified linear unit (ReLU) [39, 40] activation functions, shown in Figure 1. The output layer has five nodes, yielding a probability for each of the five classes through a softmax activation function. We refer to this network as the baseline floating-point model.

3 QUANTIZATION-AWARE PRUNING

Applying quantization and pruning to a NN can drastically improve its efficiency with little to no loss in performance. While applying these changes to a model post-training can be successful, to be maximally effective, we consider these effects at the time of NN training. Because computational complexity, as defined in Sec. 4, is quadratically dependent on precision while it is linearly dependent on pruning, the first

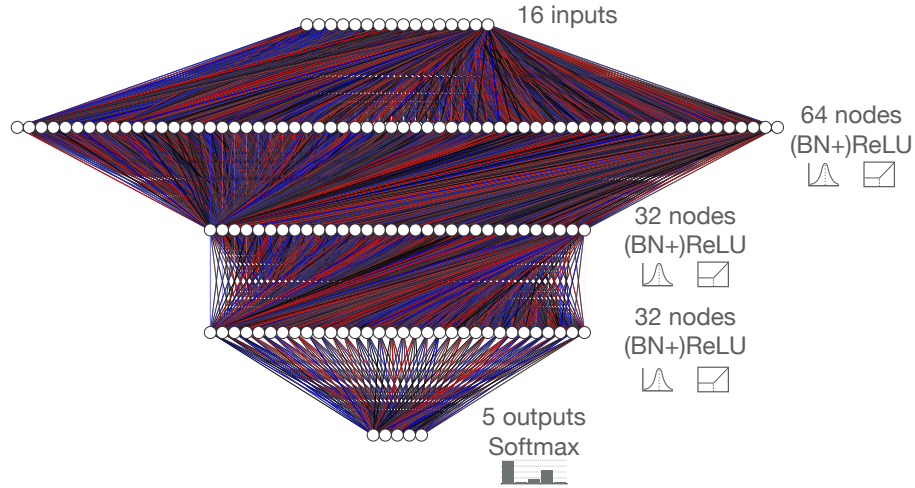


Figure 1. Baseline fully-connected neural network architecture, consisting of 16 inputs, five softmax-activated outputs, and three hidden layers. The three hidden layers contain 64, 32, and 32 hidden nodes each with ReLU activation. A configuration with batch normalization (BN) layers before each ReLU activation function is also considered. The red and blue lines represent positive and negative weights, respectively, and the opacity represents the magnitude of each weight for this randomly initialized network.

step in our QAP approach is to perform QAT. This is followed by integrating pruning in the procedure.

3.1 Quantization-aware training

Quantized [18, 41–45] and even binarized [14, 44, 46–49] NNs have been studied as a way to compress NNs by reducing the number of bits required to represent each weight and activation value. As a common platform for NNs acceleration, FPGAs provide considerable freedom in the choice of data type and precision. Both choices should be considered carefully to prevent squandering FPGA resources and incurring additional latency. For example, in QKERAS and hls4ml [8], a tool for transpiling NNs on FPGAs, fixed-point arithmetic is used, which requires less resources and has a lower latency than floating-point arithmetic. For each parameter, input, and output, the number of bits used to represent the integer and fractional parts can be configured separately. The precision can be reduced through PTQ, where pre-trained model parameters are clipped or rounded to lower precision, without causing a loss in performance [44] by carefully choosing the bit precision.

Compared to PTQ, a larger reduction in precision can be achieved through QAT [13, 50, 16], where the reduced precision of the weights and biases are accounted for directly in the training of the NN. It has been found that QAT models can be more efficient than PTQ models while retaining the same performance [24]. In these studies, the same type of quantization is applied everywhere. More recently [51, 28, 29], it has been suggested that per-layer heterogeneous quantization is the optimal way to achieve high accuracy at low resource cost. For the particle physics task with a fully-connected NN, the accuracy of the reduced precision model is compared to the 32-bit floating-point implementation as the bit width is scanned. In the PTQ case [8], the accuracy begins to drop below 14-bit fixed-point precision, while in the QAT case implemented with QKERAS [24] the accuracy is consistent down to 6 bits.

In this work, we take a different approach to training quantized NNs using BREVITAS [27], a PYTORCH library for QAT. BREVITAS provides building blocks at multiple levels of abstraction to compose and apply quantization primitives at training time. The goal of BREVITAS is to model the data type restrictions

imposed by a given target platform along the forward pass. Given a set of restriction, BREVITAS provides several alternative learning strategies to fulfill them, which are exposed to the user as hyperparameters. Depending on the specifics of the topology and the overall training regimen, different learning strategies can be more or less successful at preserving the accuracy of the output NN. Currently, the available quantizers target variations of binary, ternary, and integer data types. Specifically, given a real valued input x , the integer quantizer $Q_{\text{int}}(x)$ performs uniform affine quantization, defined as

$$Q_{\text{int}}(x) = s \underset{y_{\min}, y_{\max}}{\text{clamp}} \left(\text{round} \left(\frac{x}{s} \right) \right) \quad (1)$$

where

$$\underset{y_{\min}, y_{\max}}{\text{clamp}}(y) = \begin{cases} y_{\min} & y < y_{\min}, \\ y & y_{\min} \leq y \leq y_{\max}, \\ y_{\max} & y > y_{\max}, \end{cases} \quad (2)$$

$\text{round}(\cdot) : \mathbb{R} \rightarrow \mathbb{Z}$ is a rounding function, $s \in \mathbb{R}$ is the *scale factor*, and $y_{\min} \in \mathbb{Z}$ and $y_{\max} \in \mathbb{Z}$ are the minimum and maximum thresholds, respectively, which depend on the available word length (number of bits in a word).

In this work, we adopt round-to-nearest as the round function, and perform per-tensor quantization on both weights and activations, meaning that s is constrained to be a scalar floating-point value. As the ReLU activation function is used throughout, unsigned values are used for quantized activations. Thus, for a word length of n , the clamp function, $\text{clamp}_{A_{\min}, A_{\max}}(\cdot)$, is used with $A_{\min} = 0$ and $A_{\max} = 2^n - 1$. Quantized weights are constrained to symmetric signed values so $\text{clamp}_{w_{\min}, w_{\max}}(\cdot)$ is used with $w_{\max} = 2^{n-1} - 1$ and $w_{\min} = -w_{\max}$.

In terms of learning strategies, we apply the straight-through estimator (STE) [14] during the backward pass of the rounding function, which assumes that quantization acts as the identity function, as is typically done in QAT. For the weights' scale, similar to Ref. [52], s_w is re-computed at each training step such that the maximum value in each weight tensor is represented exactly

$$s_w = \frac{\max_{\text{tensor}}(|\mathbf{W}|)}{2^{n-1} - 1}, \quad (3)$$

where \mathbf{W} is the weight tensor for a given layer and $\max_{\text{tensor}}(\cdot)$ is the function that takes an input tensor and returns the maximum scalar value found within. For the activations, the scale factor s_A is defined as:

$$s_A = \frac{s_{A, \text{learned}}}{2^{n-1}}, \quad (4)$$

where $s_{A, \text{learned}}$ is a parameter individual to each quantized activation layer, initialized to 6.0 (in line with the ReLU6(\cdot) activation function), and learned by backpropagation in logarithmic scale, as described in Ref. [53]. In the following, we refer to this scheme as scaled-integer quantization.

3.2 Integrating pruning

Network compression is a common technique to reduce the size, energy consumption, and overtraining of deep NNs [45]. Several approaches have been successfully deployed to compress networks [54–56]. Here we focus specifically on *parameter pruning*: the selective removal of weights based on a particular ranking [4, 5, 7, 45, 57, 58].

Prior studies [8] have applied pruning in an iterative fashion: by first training a model then removing a fixed fraction of weights per layer then retraining the model, while masking the previously pruned weights. This process can be repeated, restoring the final weights from the previous iteration, several times until reaching the desired level of compression. We refer to this method as fine-tuning (FT) pruning. While the above approach is effective, we describe here an alternative approach based on the LT hypothesis [4] where the remaining weights after each pruning step are initialized back to their original values (“weight rewinding”). We refer to this method as LT pruning. We propose a new hybrid method for constructing efficient NNs, QAP, which combines a pruning procedure with training that accounts for quantized weights. As a first demonstration, we use BREVITAS [27] to perform QAT and iteratively prune a fraction of the weights following the FT pruning method. In this case, we FT prune approximately 10% of the original network weights (about 400 weights) each iteration, with a reduction in the number of weights to prune once a sparsity of 90% is reached. Weights with the smallest L_1 norms across the full model are removed each iteration.

Our procedure for FT and LT pruning are demonstrated in Figure 2, which shows the training and validation loss as a function of the epoch. To demonstrate the effect of QAP, we start by training a network using QAT for our jet substructure task constraining the precision of each layer to be 6 bits using BREVITAS. This particular training includes batch normalization (BN) layers and L_1 regularization described in more detail in Sec. 3.3, although we also present results without these aspects.

In Figure 2 (left), the FT pruning procedure iteratively prunes the 6-bit weights from the network. Each iteration is denoted by the dotted red lines after which roughly 10% of the lowest magnitude weights are removed. At each iteration, we train for 250 epochs with an early stopping criteria of no improvement in the validation loss for 10 epochs. The FT pruning procedure continues to minimize or maintain the same loss over several pruning iterations until the network becomes so sparse that the performance degrades significantly around epoch 300. In Figure 2 (right), the LT pruning procedure is shown. Our approach deviates from the canonical LT pruning study [4] in that we fully train each pruning iteration until the early stopping criteria is satisfied instead of partially optimizing the network. This is because we would like to explore the performance of the network at each stage of pruning to evaluate a number of metrics. However, the behavior is as expected—at each pruning iteration the loss goes back to its initial value. We note that because of the additional introspection at each iteration, our LT pruning procedure requires many more epochs to train than the FT pruning procedure.

3.3 Neural network training configurations

In this section, we describe BN and L_1 regularization, which have the power to modify the efficiency of our QAP models. We also describe Bayesian optimization (BO), which we use to perform a standard neural architecture search for comparison to QAP.

3.3.1 Batch normalization and L_1 regularization

BN [59] was originally proposed to mitigate internal covariate shift, although others have suggested its true benefit is in improving the smoothness of the loss landscape [60]. The BN transformation y for an input x is

$$y = \gamma \frac{x - \mu}{\sqrt{\sigma^2 + \epsilon}} + \beta, \quad (5)$$

given the running mean μ and standard deviation σ , the learnable scale γ and shift β parameters, and ϵ a small number to increase stability. Practically, the BN layer shifts the output of dense layers to the range

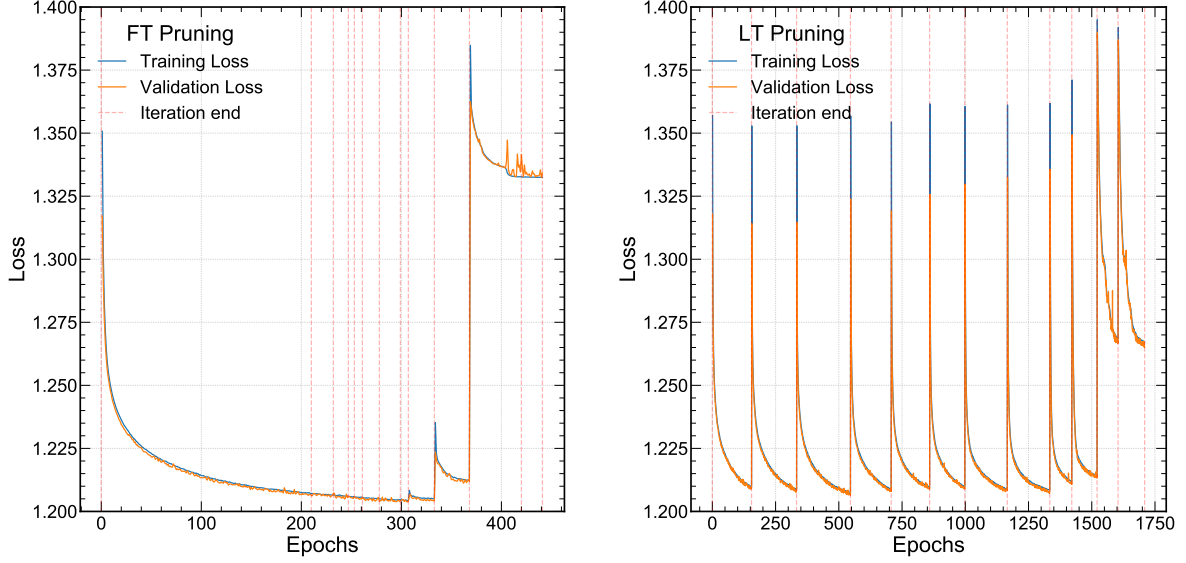


Figure 2. The loss function for the QAP procedure for a 6-bit jet classification neural network. FT pruning is demonstrated on the left and LT pruning is shown on the right.

of values in which the activation function is nonlinear, enhancing the network’s capability of modeling nonlinear responses, especially for low bit precision [23, 50]. For this reason, it is commonly used in conjunction with extremely low bit precision.

We also train models with and without L_1 regularization [8, 45, 61], in which the classification loss function L_c is augmented with an additional term,

$$L = L_c + \lambda \|w\|_1, \quad (6)$$

where w is a vector of all the weights of the model and λ is a tunable hyperparameter. This can be used to assist or accelerate the process of iterative pruning, as it constrains some weights to be small, producing already sparse models [62]. As the derivative of the penalty term is λ whose value is independent of the weight, L_1 regularization can be thought of as a force that subtracts some constant from an ineffective weight each update until the weight reaches zero.

3.3.2 Bayesian optimization

BO [63–65] is a sequential strategy for optimizing expensive-to-evaluate functions. In our case, we use it to optimize the hyperparameters of the neural network architecture. BO allows us to tune hyperparameters in relatively few iterations by building a smooth model from an initial set of parameterizations (referred to as the “surrogate model”) in order to predict the outcomes for as yet unexplored parameterizations. BO builds a smooth surrogate model using Gaussian processes (GPs) based on the observations available from previous rounds of experimentation. This surrogate model is used to make predictions at unobserved parameterizations and quantify the uncertainty around them. The predictions and the uncertainty estimates are combined to derive an acquisition function, which quantifies the value of observing a particular parameterization. We optimize the acquisition function to find the best configuration to observe, and then after observing the outcomes at that configuration a new surrogate model is fitted. This process is repeated until convergence is achieved.

We use the Ax and BoTorch libraries [66–68] to implement the BO based on the expected improvement (EI) acquisition function,

$$\text{EI}(x) = \mathbb{E}[\min(f(x) - f^*, 0)] , \quad (7)$$

where $f^* = \min_i y_i$ is the current best observed outcome and our goal is to minimize f . The total number of trials is set to 20 with a maximum number of parallel trials of 3 (after the initial exploration). Our target performance metric is the binary cross entropy loss as calculated on a “validation” subset of the jet substructure dataset. After the BO procedure is complete, and a “best” set of hyperparameters is found, each set of hyperparameters tested during the BO procedure is then fully trained for 250 epochs with an early stopping condition, and then metrics are calculated for each model on the “test” subset of the jet substructure dataset.

4 EVALUATION METRICS

As we develop NN models to address our benchmark application, we use various metrics to evaluate the NNs’ performance. Traditional metrics for performance include the classification accuracy, the receiver operating characteristic (ROC) curve of false positive rate versus true positive rate and the corresponding area under the curve (AUC). In physics applications, it is also important to evaluate the performance in the tails of distributions and we will introduce metrics to measure that as well. The aim of quantization and pruning techniques is to reduce the energy cost of neural network implementations, and therefore, we need a metric to measure the computational complexity. For this, we introduce a modified version of BOPs [34]. In addition, in this study we aim to understand how the network itself changes during training and optimization based on different neural network configurations. While the performance may be similar, we would like to understand if the information is organized in the neural network in the same way. Then we would like to understand if that has some effect on robustness of the model. To that end, we explore Shannon entropy metrics [69] and performance under class randomization.

4.1 Classification performance

For our jet substructure classification task, we consider the commonly-used accuracy metric to evaluate for the multi-class performance: average accuracy across the five jet classes. Beyond that, we also want to explore the full shape of the classifier performance in the ROC curve. This is illustrated in Fig. 3 where the signal efficiency of each signal class is plotted against the misidentification probability for the other four classes, denoted as the background efficiency. In particle physics applications, it is common to search for rare events so understanding tail performance of a classifier is also important. Therefore, as another performance metric, we define the background efficiency at a fixed signal efficiency of 50%, $\epsilon_b^{\epsilon_s=0.5}$. We can report this metric $\epsilon_b^{\epsilon_s=0.5}$ for any signal type, considering all other classes as background processes. In Fig. 3, we show the ROC curves for two NN models: one trained with 32-bit floating-point precision and another one trained with QAT at 6-bit scaled-integer precision. The networks are trained with L_1 regularization and BN layers and do not include pruning.

4.2 Bit operations

The goal of quantization and pruning is to increase the efficiency of the NN implementation in hardware. To estimate the NN computational complexity, we use the BOPs metric [34]. This metric is particularly relevant when comparing the performance of mixed precision arithmetic in hardware implementations on FPGAs and ASICs. We modify the BOPs metric to include the effect of unstructured pruning. For a pruned

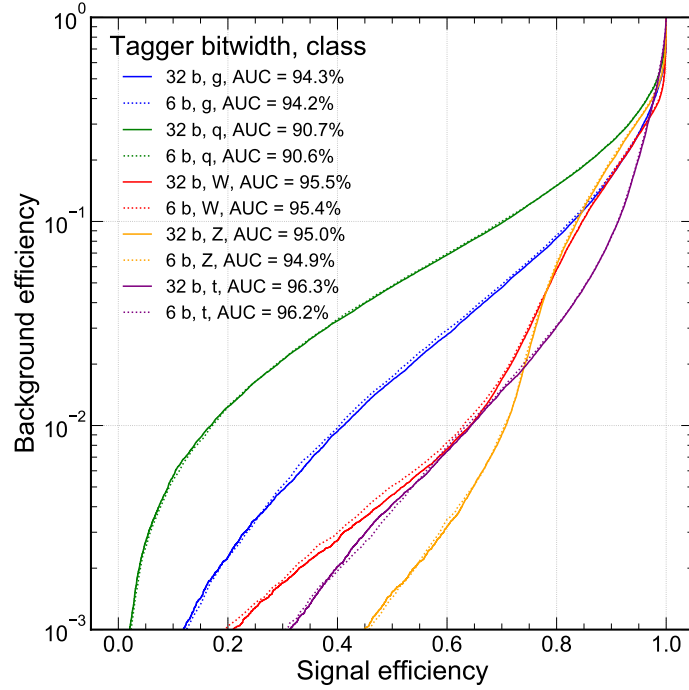


Figure 3. The ROC curve for the unpruned 32-bit floating point and 6-bit scaled integer models, trained with batch normalization layers and L_1 Regularization

fully-connected layer, we define it as

$$\text{BOPs} = mn [(1 - f_p)b_a b_w + b_a + b_w + \log_2(n)] \quad (8)$$

where n (m) is the number of inputs (outputs), b_w (b_a) is the bit width of the weights (activations), and f_p is the fraction of pruned layer weights. The inclusion of the f_p term accounts for the reduction in multiplication operations because of pruning. In the dominant term, due to multiplication operations ($b_a b_w$), BOPs is quadratically dependent on the bit widths and linearly dependent on the pruning fraction. Therefore, reducing the precision is the first step in our QAP procedure, as described above, followed by iterative pruning.

4.3 Shannon entropy, neural efficiency, and generalizability

Typically, the hardware-centric optimization of a NN is a multi-objective, or Pareto, optimization of the algorithm performance (in terms of accuracy or AUC) and the computational cost. Often, we can arrive at a range of Pareto optimal solutions through constrained minimization procedures. However, we would like to further understand how the *information* in different hardware-optimized NN implementations are related. For example, do solutions with similar performance and computational cost contain the same information content? To explore that question, we use a metric called *neural efficiency* η_N [33].

Neural efficiency measures the utilization of state space, and it can be thought of as an entropic efficiency. If all possible states are recorded for data fed into the network, then the probability, p_s , of a state s occurring

can be used to calculate Shannon entropy E_ℓ of network layer ℓ

$$E_\ell = - \sum_{s=1}^S p_s \log_2(p_s), \quad (9)$$

where the sum runs over the total size of the state space S . For a b -bit implementation of a network layer with N_ℓ neurons, this sum is typically intractable to compute, except for extremely low bit precision and small layer size, as the state space size is $S = 2^{bN_\ell}$. Therefore, a simplification is made to treat the state of a single neuron as binary (whether the output value is greater than zero) so that $S = 2^{N_\ell}$. The maximum entropy of a layer corresponds to the case when all states occur with equal probability, and the entropy value is equal to the number of neurons $E_\ell = N_\ell$. The neural efficiency of a layer can then be defined as the entropy of the observed states relative to the maximum entropy: $\eta_\ell = E_\ell / N_\ell$. Neuron layers with neural efficiency close to one (zero) are making maximal (minimal) usage of the available state space. Alternatively, high neural efficiency could also mean the layer contains too few neurons.

To compute the neural efficiency of a fully-connected NN η_N we take the geometric mean of the neural efficiency of each layer η_ℓ in the network

$$\eta_N = \left(\prod_{\ell=1}^L \eta_\ell \right)^{\frac{1}{L}} \quad (10)$$

Although neural efficiency η_N does not directly correlate with NN performance, in Ref. [33], it was found there was connection between NN generalizability and the neural efficiency. NNs with higher neural efficiency that maintain good accuracy performance were able to perform better when classes were partially randomized during training. The interpretation is that such networks were able to learn general features of the data rather than memorize images and therefore are less susceptible to performance degradation under class randomization. Therefore, in the results of our study, we also explore the effect of class randomization on our jet substructure task.

5 RESULTS

In this section, we explore how the QAP procedure described previously performs under various NN configurations. In Section 5.1, we study the effect of regularization and BN on performance metrics, accuracy and $\epsilon_b^{\epsilon_s=0.5}$, introduced in Section 4.1. We also compare the LT and FT pruning procedures. To compare the sparse NNs optimized using QAP with dense NNs, we perform QAT without pruning and choose the layer widths using BO in Section 5.2. In Section 5.3, we explore the information content of our trained NNs using neural efficiency as a metric. We also investigate how that content varies under class randomization as a measure of the generalizability.

5.1 QAP performance

The physics classifier performance is measured with the accuracy and $\epsilon_b^{\epsilon_s=0.5}$ metric for each signal class. We train a number of models at different precision: 32-bit floating-point precision and 12-, 6-, and 4-bit scaled-integer precision. For each precision explored, we then apply a pruning procedure. We explore both of the LT and FT pruning schemes described in Section 3. The result is illustrated in Figure 4 where each of the colored lines indicates a different model precision, the solid (dashed) lines correspond to FT (LT) pruning, and each of the points along the curves represents the percent of the original network weights

that have been pruned. Each NN includes a BN layer after each of the hidden layers and has been trained including an L_1 regularization loss term. Further, each model's performance was verified via a k -fold cross-validation scheme, where $k = 4$ in which training and validation datasets were shuffled over multiple training instances. Plotted performance is the mean value and error bars represent the standard error across the folds. All metrics were calculated on the same test dataset, which stayed static across each training instance.

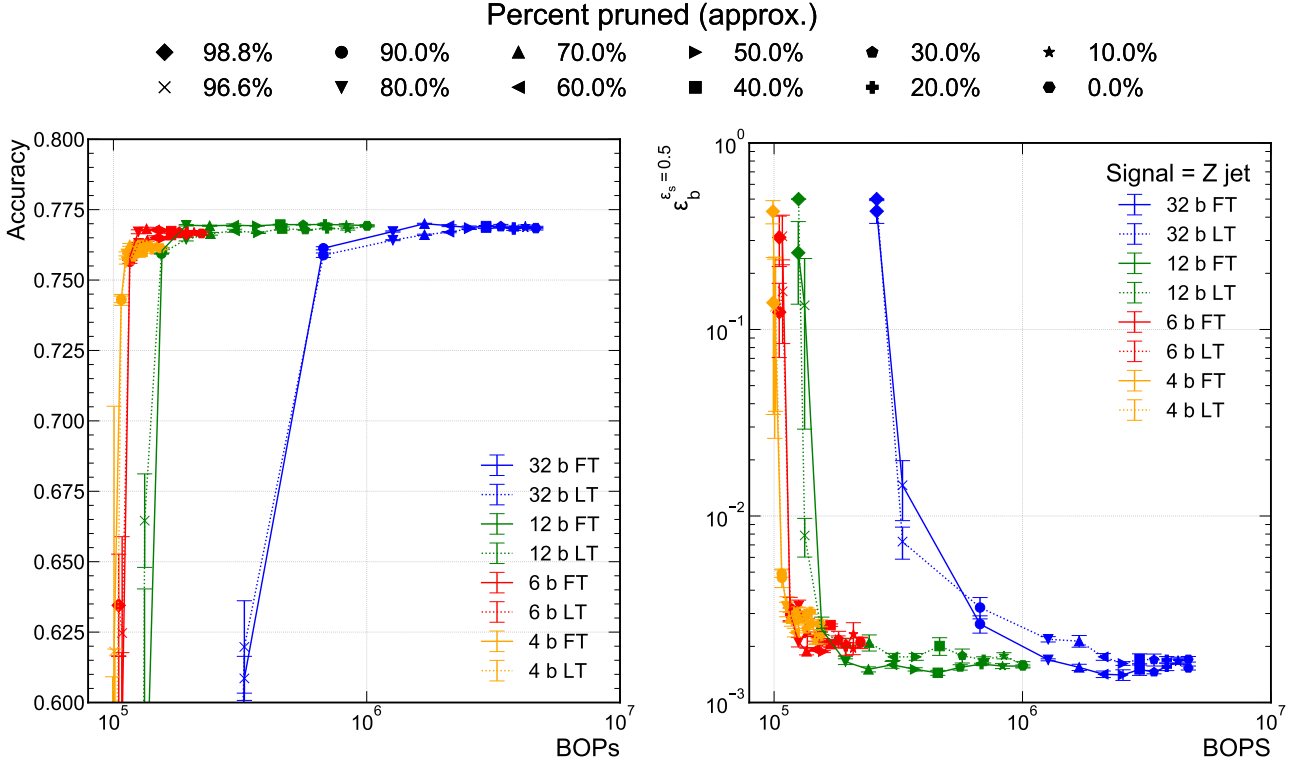


Figure 4. Model accuracy and background efficiency at 50% signal efficiency versus BOPs for different sparsities achieved via QAP, for both FT and LT pruning techniques

The first observation from Figure 4 is that we can achieve comparable performance to the 32-bit floating-point model with the 6-bit scaled-integer model. This is consistent with findings in a previous QKERAS-based study [24] where, with uniform quantization, the performance was consistent down to 6-bit fixed-point quantization. When the precision is reduced to 4-bits, the performance begins to degrade. Then, as we increasingly prune the models at all of the explored precisions, the performance is maintained until about 80% of the weights are pruned. The observations are consistent whether we consider the accuracy (Figure 4 left) or $\epsilon_b^{\epsilon_s=0.5}$ (Figure 4 right) metric. In the case of $\epsilon_b^{\epsilon_s=0.5}$, there are statistical fluctuations in the values because of the limited testing sample size and the small background efficiencies of 2×10^{-3} that we probe. If we compare the performance of our QAP 6-bit model to the unpruned 32-bit model, we find a greater than $25\times$ reduction in computational cost (in terms of BOPs) for the same classifier performance. For the jet substructure classification task, the quantization and pruning techniques are complementary and can be used in tandem at training time to develop an extremely efficient NN. With respect to earlier work with FT pruning at 32-bit floating-point precision and PTQ presented in Ref. [8], we find a further greater than $3\times$ reduction in BOPs.

In Fig. 4, we also find that there is no significant performance difference between using FT and LT pruning. As we prune the networks to extreme sparsity, greater than 80%, the performance begin to degrade drastically for this particular dataset and network architecture. While the plateau region is fairly stable, in the ultra-sparse region, there are significant variations in the performance metrics indicating that the trained networks are somewhat brittle. For this reason, we truncate the accuracy versus BOPs graphs at 60% accuracy.

We also explore the performance of the model when removing either the BN layers or the L_1 regularization term, which we term the *no BN* and *no L_1* models, respectively. This is illustrated in Fig. 5 for the 32-bit floating-point and 6-bit scaled-integer models. For easier visual comparisons, we omit the 4-bit and 12-bit models because the 6-bit model is the lowest precision model with comparable performance to the 32-bit model. In Fig. 5 (left), we see that there is a modest performance degradation in the no BN configuration for both lower and full precision models. In our application, we find that batch normalization does stabilize and improve the performance of our neural network and thus include it in our baseline model definition. In Fig. 5 (right), we find that including or removing the L_1 regularization term in the loss function does not affect the performance significantly until extreme sparsity where the variations in performance can be large. However, as we will see in Section 5.3, this does not mean that the entropic information content of the NNs are similar.

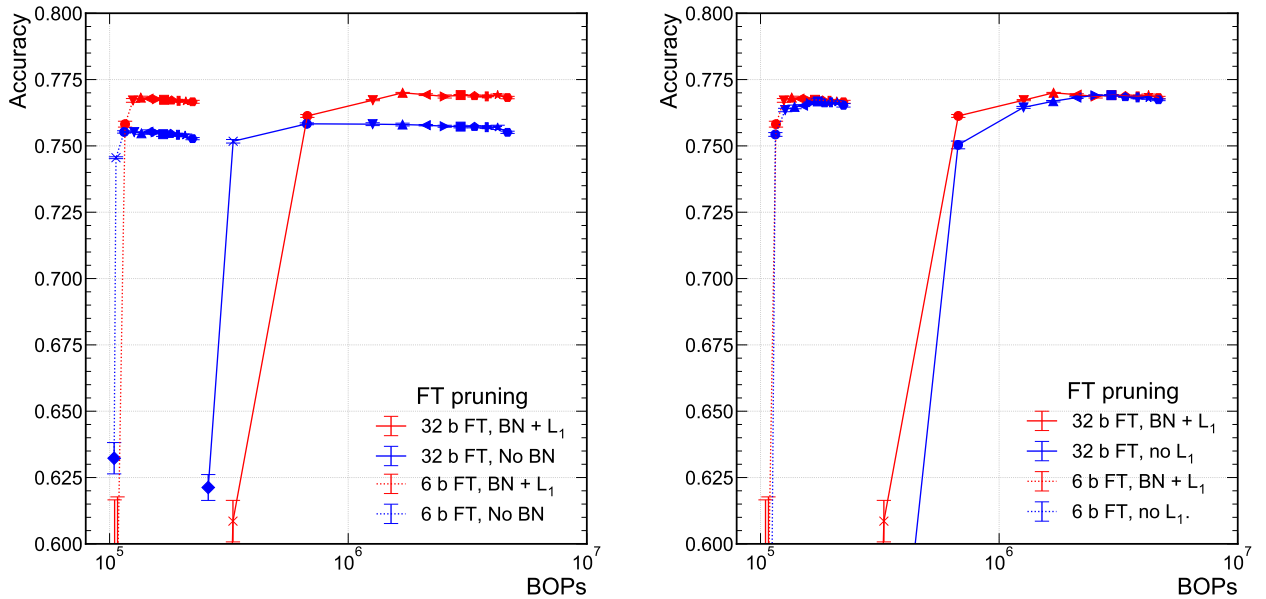


Figure 5. Comparison of the model accuracy when trained with BN layers and L_1 regularization versus when trained without BN layers or L_1 regularization.

To highlight the performance of the QAP procedure, we summarize our result compared to previous results for this jet substructure classification task with the same NN architecture shown in Figure 1. The results are summarized in Table 1. In the nominal implementation, no quantization or pruning is performed. In Ref. [8], the 32-bit floating-point model is FT pruned and then quantized post-training. This approach suffers from a loss of performance below 16 bits. Using QAT and QKERAS [24], another significant improvement was demonstrated with a 6-bit fixed-point implementation. Finally, in this work with QAP and BREVITAS, we are able to prune the 6-bit network by another 80%. With respect to the nominal

implementation we have reduced the BOPs by a factor of 25, the original pruning + PTQ approach a factor of 3.3, and the QAT approach by a factor of 2.2.

One further optimization step is to compare against a mixed-precision approach where different layers have different precisions [24]. We leave the study of mixed-precision QAP to future work and discuss it in Section 6.

Model	Precision	BN or L_1	Pruned [%]	BOPs	Accuracy [%]
Nominal	32-bit floating-point	BN + L_1	0	4,652,832	76.977
Pruning + PTQ	16-bit fixed-point	BN + L_1	70	631,791	75.035
QAT	6-bit fixed-point	BN + L_1	0	412,960	76.737
QAP	6-bit scaled-integer	BN + L_1	80	189,672	76.602

Table 1. Performance evolution of the jet substructure classification task for this NN architecture. “Nominal” refers to an unpruned 32-bit implementation, “pruning + PTQ” refers to a network with FT pruning at 32-bit precision with PTQ applied to reduce the precision to 16 bits, “QAT” refers to a QKERAS implementation, and “QAP” is this result.

5.2 Pruned versus unpruned quantized networks

To compare against the efficacy of applying QAP, we explore QAT with no pruning. In an alternate training strategy, we attempt to optimize the NN architecture of the unpruned QAT models. This is done using the BO technique presented in Section 3.3. The widths of the hidden layers are varied to find optimal classifier performance. We compare the performance of this class of possible models using BO against our QAP procedure, including BN and L_1 regularization, presented in the previous section. It is important to note, as we will see, that QAP and BO are conceptually different procedures and interesting to compare. The QAP procedure starts with a particular accuracy-optimized model and attempts to “streamline” or compress it to its most optimal bit-level implementation. This is the reason that the accuracy drops precipitously when that particular model can no longer be streamlined. Alternatively, the family of BO models explores the Pareto optimal space between BOPs and accuracy. In future work, we would like to further explore the interplay between QAP and BO.

Figure 6 presents both the accuracy versus BOPs curves for the QAP models and the unpruned QAT models found using BO. For ease of comparison, we display only the 32-bit and 6-bit models. The solid curves correspond to the QAP models while the individual points represent the various trained unpruned models explored during the BO procedure. The unpruned model with the highest classification performance found using the BO procedure is denoted by the star. While the starred models are the most performant, there is a class of BO models that tracks along the QAP curves fairly well. There is a stark difference in how QAP and BO models behave as the accuracy degrades below the so-called “plateau” region where the accuracy is fairly constant and optimal. When the sub-network of the QAP model can no longer approximate the optimally performing model, its performance falls off dramatically and the accuracy drops quickly. Because BO explores the full space including Pareto optimal models in BOPs versus accuracy, they exhibit a more gentle decline in performance at small values of BOPs. It is interesting to note that the classification performance of the BO models begins to degrade where the QAP procedure also falls off in performance; for example, just above 10^5 /BOPs in Fig. 6 (left) for the 6-bit models. We anticipate future work to explore combining BO and QAP procedures to see if any accuracy optimal model can be found at smaller BOPs values.

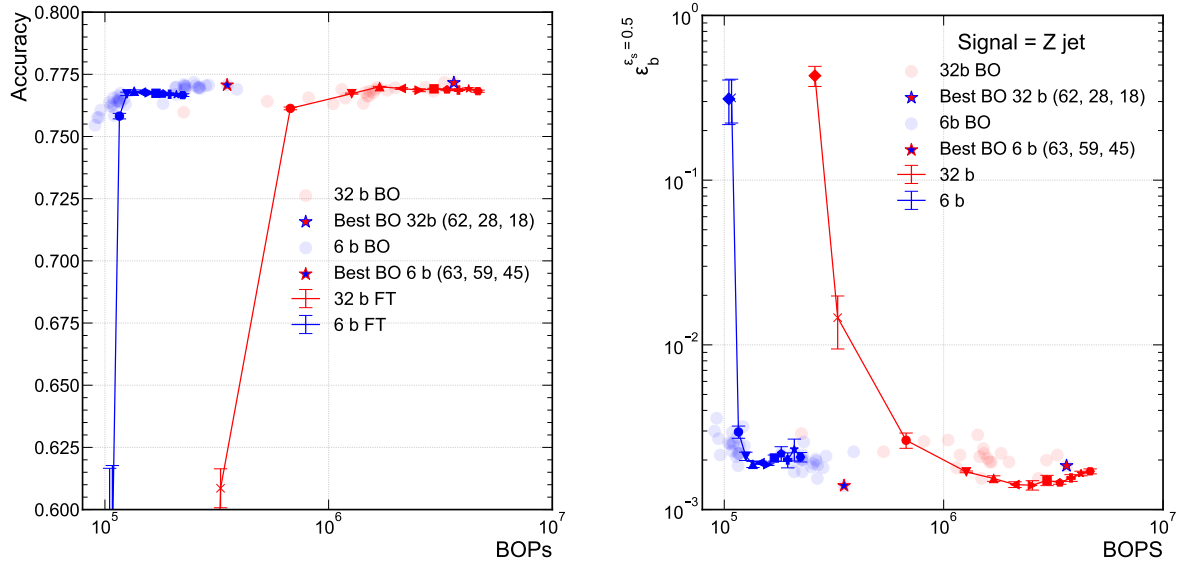


Figure 6. Comparison of FT pruned model’s and BO model’s accuracy and background efficiency at 50% signal efficiency. Each hyperparameter configuration that was explored during the BO procedure is marked as a transparent dot, with the resulting “best” model, which the lowest BCE Loss as calculated on the “test” set, is marked by the outlined star

5.3 Entropy and generalization

QAP models exhibit large gains in computational efficiency over (pruned and unpruned) 32-bit floating-point models, as well as significant gains over unpruned QAT models for our jet substructure classification task. In certain training configurations, we have found similar performance but would like to explore if the information in the neural network is *represented* similarly. As a metric for the information content of the NN, we use the *neural efficiency* metric defined in Equation (10), the Shannon entropy normalized to the number of neurons in a layer then averaged over all the layers of the NN.

By itself, the neural efficiency is an interesting quantity to measure. However, we specifically explore the hypothesis, described in Section 4, that the neural efficiency is related to a measure of generalizability. In this study, we use the classification performance under different rates of class randomization during training as a probe of the generalizability of a model. We randomize the class labels among the five possible classes for 0%, 50%, 75%, and 90% of the training dataset.

To compare with the results in Section 5, we study models that are trained using QAP with 6-bit precision and are pruned using the fine-tuning pruning procedure. The results are presented in Figure 7 where the left column shows the classifier accuracy versus BOPs. The right column displays the neural efficiency versus BOPs. The three rows explore three different scenarios: with both BN and L_1 regularization (upper), no BN (middle), and no L_1 (lower). The various curves presented in each graph correspond to different class label randomization fractions of the training sample.

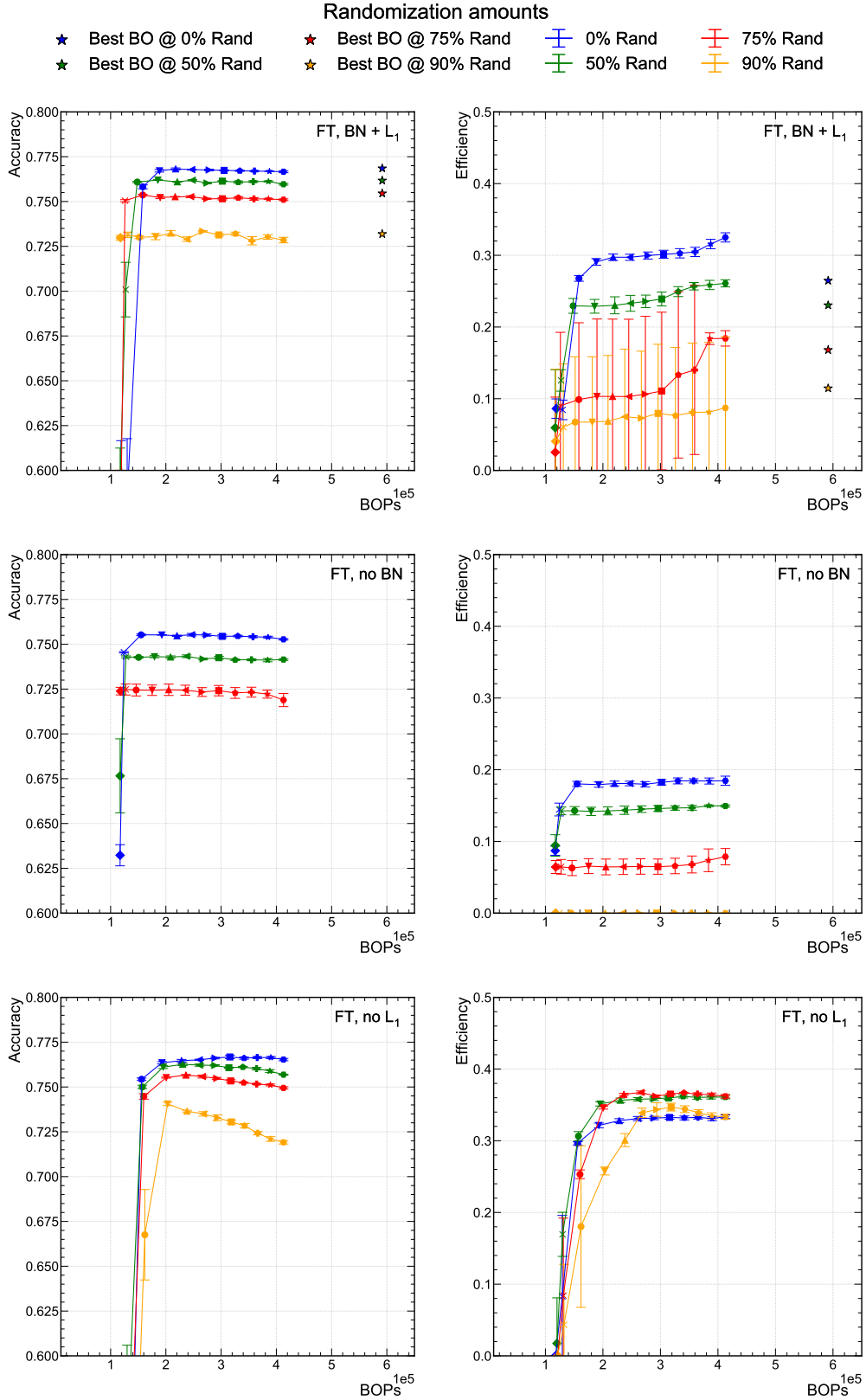


Figure 7. Comparison of accuracy and neural efficiency for a 6-bit QAP model as BN layers and/or L_1 regularization is present in the model. L_1 + BN (upper), no BN (middle), and no L_1 (lower)

Among these training procedures, the L_1 + BN model accuracy (upper left) is the highest and most consistent across the entire pruning procedure. Even with 90% class randomization, the accuracy is still greater than 72.5%. Alternatively, the no BN model accuracy is consistently worse than the L_1 + BN models for all values of randomization. Interestingly, the no BN model accuracy with 90% randomization drops precipitously out of the range of the graphs indicating that BN is even more important to performance

when class randomization is introduced. Meanwhile, the no L_1 model exhibits an interesting behavior with lower accuracy at larger values of BOPs. As the no L_1 model is pruned, the accuracy improves until we arrive at extreme sparsity and the model performance degrades as usual. Our interpretation is that the generalization power of the unregularized model is worse than the L_1 regularized models. However, as we implement the QAP procedure, the pruning effectively regularizes the model building robustness to the class randomization and recovering some of the lost accuracy.

The corresponding neural efficiency plots are shown in the right column of Figure 7. As a general observation, we find that the neural efficiency follows the same trend versus BOPs as the accuracy, i.e. that within a given training configuration, the neural efficiency is stable up to a given sparsity. Thus, up to this point, pruning does not affect the information content. This is particularly true in the case of the no BN model, while with BN there is more freedom, and thus modest variation in neural efficiency during the pruning procedure.

If we first only consider the 0% randomized models for the right column, we can see that the neural efficiency drops from about 0.3 to about 0.2 with the no BN configuration. As the neural efficiency is a measure of how balanced the neurons are activated (i.e. how efficiently the full state space is used), we hypothesize that BN more evenly distributes the activation among neurons. For the models that include L_1 regularization (upper and middle), the neural efficiency drops along with the accuracy as the randomization is increased. This effect is not nearly as strong in the no L_1 case in the lower row. We note that the performance of the 90% randomized no BN model is catastrophically degraded and the neural efficiency drops to zero, which we interpret to indicate that BN is an important factor in the robustness and generalizability of the model.

The no L_1 models (lower) are particularly notable because the neural efficiency does not decrease much as we the class randomization fraction is increased, in contrast with the upper and middle rows of Figure 7. This however, does not translate into a more robust performance. In fact, at 90% class randomization and 80% pruned, the L_1 + BN and no L_1 models are drastically different in neural efficiency while being fairly similar in classifier accuracy.

Finally, the accuracy and neural efficiency of the highest accuracy models from the BO procedure in Section 5.2 are represented as stars in the top row of Figure 7. They have slightly lower neural efficiencies because the width of each hidden layer is bigger than in the QAP models while the entropy remains relatively similar to those same models. The BO models, as seen in the upper left graph of Figure 7, are no better at generalizing under increasing class randomization fractions than the QAP models.

6 SUMMARY AND OUTLOOK

In this study, we explored efficient neural network (NN) implementations by coupling pruning and quantization at training time. Our benchmark task is ultra low latency, resource-constrained jet classification in the real-time online filtering system, implemented on field-programmable gate arrays (FPGAs), at the CERN Large Hadron Collider (LHC). This classification task takes as inputs high-level expert features in a fully-connected NN architecture.

Our procedure, called quantization-aware pruning (QAP), is a combination of quantization-aware training (QAT) followed by iterative unstructured pruning. This sequence is motivated by the fact that quantization has a larger impact on a model’s computational complexity than pruning as measured by bit operations (BOPs). We studied two types of pruning: fine-tuning (FT) and lottery ticket (LT) approaches. Furthermore, we study the effect of batch normalization (BN) layers and L_1 regularization on network performance. Under this procedure, considering networks with uniformly quantized weights, we found that with almost no loss in classifier accuracy, the number of BOPs can be reduced by a factor of 25, 3.3, and 2.2 with respect to the nominal 32-bit floating-point implementation, pruning with post-training quantization (PTQ), and QAT, respectively. This demonstrates that, for our task, pruning and QAT are complementary and can be used in concert.

Beyond computational performance gains, we sought to understand two related issues to the QAP procedure. First, we compare QAP to QAT with a Bayesian optimization (BO) procedure that optimizes the layer widths in the network. We found that the BO procedure did not find a network configuration that maintains performance accuracy with fewer BOPs and that both procedures find similarly efficiently sized networks as measured in BOPs and high accuracy.

Second, we studied the information content, robustness, and generalizability of the trained QAP models in various training configurations and in the presence of randomized class labels. We compute both the networks’ accuracies and their entropic information content, measured by the neural efficiency metric [33]. We found that both L_1 regularization and BN are required to provide the most robust NNs to class randomization. Interestingly, while removing L_1 regularization did not significantly degrade performance under class randomization, the neural efficiencies of the NNs were vastly different—varying by up to a factor of 3. This illustrates, that while NNs may arrive at a similar performance accuracy, the information content in the networks can be very different.

6.1 Outlook

As one of the first explorations of pruning coupled with quantization, our initial study of QAP lends itself to a number of follow-up studies.

- Our benchmark task uses high-level features, but it is interesting to explore other canonical datasets, especially those with raw, low-level features. This may yield different results, especially in the study of generalizability.
- Combining our approach with other optimization methods such as Hessian-based quantization [28, 29] and pruning could produce networks with very different NNs in information content or more optimal solutions, particularly as the networks become very sparse.
- An important next step is evaluating the actual hardware resource usage and latency of the QAP NNs by using FPGA co-design frameworks like `hls4ml` [8] and FINN [70, 26].
- It would be interesting to explore the differences between seemingly similar NNs beyond neural efficiency; for example, using metrics like singular vector canonical correlation analysis (SVCCA) [71] which directly compare two NNs
- We would like to explore further optimal solutions by combining BO and QAP procedures. Beyond that, there is potential for more efficient solutions using mixed-precision QAT, which could be done through a more general BO procedure that explores the full space of layer-by-layer pruning fractions, quantization, and sizes.

QAP is a promising technique to build efficient NN implementations and would benefit from further study on additional benchmark tasks. Future investigation of QAP, variations on the procedure, and combination with complementary methods may lead to even greater NN efficiency gains and may provide insights into what the NN is learning.

ACKNOWLEDGMENTS

We acknowledge the Fast Machine Learning collective as an open community of multi-domain experts and collaborators. This community was important for the development of this project. Thanks especially to Duc Hoang for enabling evaluations of post-training quantized PYTORCH models using `hls4ml`. We would also like to thank Nick Schaub and Nate Hotaling from NCATS/Axel Informatics for their insight on aIQ.

B. H. and N. T. are supported by Fermi Research Alliance, LLC under Contract No. DE-AC02-07CH11359 with the U.S. Department of Energy (DOE), Office of Science, Office of High Energy Physics and the DOE Early Career Research program under Award No. DE-0000247070. J. D. is supported by the DOE, Office of Science, Office of High Energy Physics Early Career Research program under Award No. DE-SC0021187.

This work was performed using the Pacific Research Platform Nautilus HyperCluster supported by NSF awards CNS-1730158, ACI-1540112, ACI-1541349, OAC-1826967, the University of California Office of the President, and the University of California San Diego's California Institute for Telecommunications and Information Technology/Qualcomm Institute. Thanks to CENIC for the 100 Gpbs networks.

REFERENCES

- [1] Sze V, Chen YH, Yang TJ, Emer JS. Efficient processing of deep neural networks. *Synthesis Lectures on Computer Architecture* **15** (2020) 1–341.
- [2] LeCun Y, Denker JS, Solla SA. Optimal brain damage. Touretzky DS, editor, *Advances in Neural Information Processing Systems 2* (Morgan-Kaufmann) (1990), 598.
- [3] Han S, Mao H, Dally WJ. Deep compression: Compressing deep neural networks with pruning, trained quantization and huffman coding. *4th International Conference on Learning Representations* (2016).
- [4] Frankle J, Carbin M. The lottery ticket hypothesis: Training pruned neural networks. *7th International Conference on Learning Representations* (2019).
- [5] Renda A, Frankle J, Carbin M. Comparing rewinding and fine-tuning in neural network pruning. *8th International Conference on Learning Representations* (2020).
- [6] Zhou H, Lan J, Liu R, Yosinski J. Deconstructing lottery tickets: Zeros, signs, and the supermask. Wallach H, Larochelle H, Beygelzimer A, d’Alché Buc F, Fox E, Garnett R, editors, *Advances in Neural Information Processing Systems* (Curran Associates, Inc.) (2019), vol. 32, 3597.
- [7] Blalock D, Ortiz JJG, Frankle J, Gutttag J. What is the state of neural network pruning? *4th Conference on Machine Learning and Systems* (2020).
- [8] Duarte J, Han S, Harris P, Jindariani S, Kreinar E, Kreis B, et al. Fast inference of deep neural networks in FPGAs for particle physics. *J. Instrum.* **13** (2018) P07027. doi:10.1088/1748-0221/13/07/P07027.
- [9] Nagel M, van Baalen M, Blankevoort T, Welling M. Data-free quantization through weight equalization and bias correction. *2019 IEEE/CVF International Conference on Computer Vision (ICCV)* (2019), 1325. doi:10.1109/ICCV.2019.00141.
- [10] Meller E, Finkelstein A, Almog U, Grobman M. Same, same but different: Recovering neural network quantization error through weight factorization. *Proceedings of the 36th International Conference on Machine Learning (ICML)* (PMLR) (2019), vol. 97, 4486.
- [11] Zhao R, Hu Y, Dotzel J, Sa CD, Zhang Z. Improving neural network quantization without retraining using outlier channel splitting. *Proceedings of the 36th International Conference on Machine Learning (ICML)* (PMLR) (2019), vol. 97, 7543.
- [12] Banner R, Nahshan Y, Hoffer E, Soudry D. Post-training 4-bit quantization of convolution networks for rapid-deployment. Wallach H, Larochelle H, Beygelzimer A, d’Alché Buc F, Fox E, Garnett R, editors, *Advances in Neural Information Processing Systems* (Curran Associates, Inc.) (2019), vol. 32, 7950.
- [13] Moons B, Goetschalckx K, Berckelaer NV, Verhelst M. Minimum energy quantized neural networks. *2017 51st Asilomar Conference on Signals, Systems, and Computers* (2017), 1921. doi:10.1109/ACSSC.2017.8335699.
- [14] Courbariaux M, Bengio Y, David JP. BinaryConnect: Training deep neural networks with binary weights during propagations. Cortes C, Lawrence ND, Lee DD, Sugiyama M, Garnett R, editors, *Advances in Neural Information Processing Systems* (Curran Associates, Inc.) (2015), vol. 28, 3123.
- [15] Zhang D, Yang J, Ye D, Hua G. LQ-nets: Learned quantization for highly accurate and compact deep neural networks. *Proceedings of the European Conference on Computer Vision (ECCV)* (2018), 365.
- [16] Li F, Liu B. Ternary weight networks (2016).
- [17] Zhou S, Wu Y, Ni Z, Zhou X, Wen H, Zou Y. DoReFa-Net: Training low bitwidth convolutional neural networks with low bitwidth gradients (2016).
- [18] Hubara I, Courbariaux M, Soudry D, El-Yaniv R, Bengio Y. Quantized neural networks: Training neural networks with low precision weights and activations. *J. Mach. Learn. Res.* **18** (2018) 1.

- [19] Rastegari M, Ordonez V, Redmon J, Farhadi A. XNOR-Net: ImageNet classification using binary convolutional neural networks. *14th European Conference on Computer Vision (ECCV)* (Cham, Switzerland: Springer International Publishing) (2016), 525. doi:10.1007/978-3-319-46493-0_32.
- [20] Micikevicius P, Narang S, Alben J, Diamos G, Elsen E, Garcia D, et al. Mixed precision training. *6th International Conference on Learning Representations* (2018).
- [21] Zhuang B, Shen C, Tan M, Liu L, Reid I. Towards effective low-bitwidth convolutional neural networks. *2018 IEEE/CVF Conference on Computer Vision and Pattern Recognition* (2018), 7920. doi:10.1109/CVPR.2018.00826.
- [22] Wang N, Choi J, Brand D, Chen CY, Gopalakrishnan K. Training deep neural networks with 8-bit floating point numbers. Bengio S, Wallach H, Larochelle H, Grauman K, Cesa-Bianchi N, Garnett R, editors, *Advances in Neural Information Processing Systems* (Curran Associates, Inc.) (2018), vol. 31, 7675.
- [23] Ngadiuba J, Guglielmo GD, Duarte J, Harris P, Hoang D, Jindariani S, et al. Compressing deep neural networks on FPGAs to binary and ternary precision with hls4ml. *Mach. Learn.: Sci. Technol.* (2020). doi:10.1088/2632-2153/aba042.
- [24] Coelho CN, Kuusela A, Zhuang H, Aarrestad T, Loncar V, Ngadiuba J, et al. Automatic deep heterogeneous quantization of deep neural networks for ultra low-area, low-latency inference on the edge at particle colliders (2020). Submitted to *Nat. Mach. Intell.*
- [25] Coelho C. QKeras (2019).
- [26] Blott M, Preusser T, Fraser N, Gambardella G, O'Brien K, Umuroglu Y. FINN-R: An end-to-end deep-learning framework for fast exploration of quantized neural networks. *ACM Trans. Reconfigurable Technol. Syst.* **11** (2018). doi:10.1145/3242897.
- [27] Pappalardo A. Xilinx/brevitas (2020). doi:10.5281/zenodo.3333552.
- [28] Dong Z, Yao Z, Gholami A, Mahoney M, Keutzer K. HAWQ: Hessian aware quantization of neural networks with mixed-precision. *2019 IEEE/CVF International Conference on Computer Vision (ICCV)* (2019), 293.
- [29] Dong Z, Yao Z, Cai Y, Arfeen D, Gholami A, Mahoney MW, et al. HAWQ-V2: Hessian aware trace-weighted quantization of neural networks. *Advances in Neural Information Processing Systems* **33** (2020).
- [30] van Baalen M, Louizos C, Nagel M, Amjad RA, Wang Y, Blankevoort T, et al. Bayesian bits: Unifying quantization and pruning. *Advances in Neural Information Processing Systems* **33** (2020).
- [31] Hacene GB, Gripon V, Arzel M, Farrugia N, Bengio Y. Quantized guided pruning for efficient hardware implementations of convolutional neural networks. *2020 18th IEEE International New Circuits and Systems Conference (NEWCAS)* (2020), 206. doi:10.1109/NEWCAS49341.2020.9159769.
- [32] Chang SE, Li Y, Sun M, Shi R, So HKH, Qian X, et al. Mix and match: A novel fpga-centric deep neural network quantization framework. *27th IEEE International Symposium on High-Performance Computer Architecture (HPCA)* (2021).
- [33] Schaub NJ, Hotaling N. Assessing intelligence in artificial neural networks (2020).
- [34] Baskin C, Schwartz E, Zheltonozhskii E, Liss N, Giryes R, Bronstein AM, et al. UNIQ: Uniform noise injection for the quantization of neural networks (2018).
- [35] Karbachevsky A, Baskin C, Zheltonozhskii E, Yermolin Y, Gabbay F, Bronstein AM, et al. Early-stage neural network hardware performance analysis. *Sustainability* (2021) 717. doi:10.3390/su13020717.
- [36] Coleman E, Freytsis M, Hinzmann A, Narain M, Thaler J, Tran N, et al. The importance of calorimetry for highly-boosted jet substructure. *J. Instrum.* **13** (2018) T01003. doi:10.1088/1748-0221/13/01/T01003.

- [37] Moreno EA, Cerri O, Duarte JM, Newman HB, Nguyen TQ, Periwal A, et al. JEDI-net: a jet identification algorithm based on interaction networks. *Eur. Phys. J. C* **80** (2020) 58. doi:10.1140/epjc/s10052-020-7608-4.
- [38] [Dataset] Pierini M, Duarte JM, Tran N, Freytsis M. `hls4ml` LHC jet dataset (150 particles) (2020). doi:10.5281/zenodo.3602260.
- [39] Nair V, Hinton GE. Rectified linear units improve restricted Boltzmann machines. *27th International Conference on Machine Learning* (Madison, WI, USA: Omnipress) (2010), 807.
- [40] Glorot X, Bordes A, Bengio Y. Deep sparse rectifier neural networks. Gordon G, Dunson D, Dudík M, editors, *14th International Conference on Artificial Intelligence and Statistics* (Fort Lauderdale, FL, USA: JMLR) (2011), vol. 15, 315.
- [41] Gong Y, Liu L, Yang M, Bourdev LD. Compressing deep convolutional networks using vector quantization (2014).
- [42] Wu J, Leng C, Wang Y, Hu Q, Cheng J. Quantized convolutional neural networks for mobile devices. *2016 IEEE Conference on Computer Vision and Pattern Recognition (CVPR)* (2016), 4820. doi:10.1109/CVPR.2016.521.
- [43] Vanhoucke V, Senior A, Mao MZ. Improving the speed of neural networks on CPUs. *Deep Learning and Unsupervised Feature Learning Workshop at the 25th Conference on Neural Information Processing Systems* (2011).
- [44] Gupta S, Agrawal A, Gopalakrishnan K, Narayanan P. Deep learning with limited numerical precision. Bach F, Blei D, editors, *32nd International Conference on Machine Learning* (Lille, France: PMLR) (2015), vol. 37, 1737.
- [45] Han S, Mao H, Dally WJ. Deep compression: Compressing deep neural network with pruning, trained quantization and huffman coding. *4th International Conference on Learning Representations* (2016).
- [46] Hubara I, Courbariaux M, Soudry D, El-Yaniv R, Bengio Y. Binarized neural networks. Lee DD, Sugiyama M, Luxburg UV, Guyon I, Garnett R, editors, *Advances in Neural Information Processing Systems* (Curran Associates, Inc.) (2016), vol. 29, 4107.
- [47] Rastegari M, Ordonez V, Redmon J, Farhadi A. Xnor-net: Imagenet classification using binary convolutional neural networks. Leibe B, Matas J, Sebe N, Welling M, editors, *ECCV 2016* (Cham, Switzerland: Springer) (2016), 525.
- [48] Merolla P, Appuswamy R, Arthur JV, Esser SK, Modha DS. Deep neural networks are robust to weight binarization and other non-linear distortions (2016).
- [49] Loncar V, et al. Compressing deep neural networks on FPGAs to binary and ternary precision with `hls4ml`. *Mach. Learn.: Sci. Technol.* (2020) 015001. doi:10.1088/2632-2153/aba042.
- [50] Courbariaux M, Bengio Y, David JP. Binaryconnect: Training deep neural networks with binary weights during propagations. Cortes C, Lawrence ND, Lee DD, Sugiyama M, Garnett R, editors, *Advances in Neural Information Processing Systems* (Curran Associates, Inc.), vol. 28 (2015), 3123.
- [51] Wang K, Liu Z, Lin Y, Lin J, Han S. HAQ: hardware-aware automated quantization. *IEEE/CVF Conference on Computer Vision and Pattern Recognition (CVPR)* (2019), 8604. doi:10.1109/CVPR.2019.00881.
- [52] Jacob B, Kligys S, Chen B, Zhu M, Tang M, Howard A, et al. Quantization and training of neural networks for efficient integer-arithmetic-only inference. *Proceedings of the IEEE Conference on Computer Vision and Pattern Recognition* (2018), 2704.
- [53] Jain SR, Gural A, Wu M, Dick CH. Trained quantization thresholds for accurate and efficient fixed-point inference of deep neural networks **2** (2020) 112.

- [54] Cheng Y, Wang D, Zhou P, Zhang T. A survey of model compression and acceleration for deep neural networks. *IEEE Signal Process. Mag.* **35** (2018) 126. doi:10.1109/MSP.2017.2765695.
- [55] Deng L, Li G, Han S, Shi L, Xie Y. Model compression and hardware acceleration for neural networks: A comprehensive survey. *Proc. IEEE* **108** (2020) 485. doi:10.1109/JPROC.2020.2976475.
- [56] Choudhary T, Mishra V, Goswami A, Sarangapani J. A comprehensive survey on model compression and acceleration. *Artif. Intell. Rev.* **53** (2020) 5113. doi:10.1007/s10462-020-09816-7.
- [57] LeCun Y, Denker JS, Solla SA. Optimal brain damage. Touretzky DS, editor, *Advances in Neural Information Processing Systems* (Morgan-Kaufmann) (1990), vol. 2, 598.
- [58] Louizos C, Welling M, Kingma DP. Learning Sparse Neural Networks through L_0 Regularization. *6th International Conference on Learning Representations* (2018).
- [59] Ioffe S, Szegedy C. Batch normalization: Accelerating deep network training by reducing internal covariate shift. Bach F, Blei D, editors, *32nd International Conference on Machine Learning* (Lille, France: PMLR) (2015), vol. 37, 448.
- [60] Santurkar S, Tsipras D, Ilyas A, Madry A. How does batch normalization help optimization? Bengio S, Wallach H, Larochelle H, Grauman K, Cesa-Bianchi N, Garnett R, editors, *Advances in Neural Information Processing Systems* (Curran Associates, Inc.) (2018), vol. 31, 2483.
- [61] Han S, Pool J, Tran J, Dally WJ. Learning both weights and connections for efficient neural networks. Cortes C, Lawrence N, Lee D, Sugiyama M, Garnett R, editors, *Advances in Neural Information Processing Systems* (Curran Associates, Inc.) (2015), vol. 28, 1135.
- [62] Ng AY. Feature selection, L1 vs. L2 regularization, and rotational invariance. *21st International Conference On Machine Learning* (New York, NY, USA: ACM) (2004), ICML '04, 78. doi:10.1145/1015330.1015435.
- [63] Jones DR, Schonlau M, Welch WJ. Efficient global optimization of expensive black-box functions. *J. Global Optim.* **13** (1998) 455. doi:10.1023/A:1008306431147.
- [64] O'Hagan A. Curve fitting and optimal design for prediction. *J. Royal Stat. Soc. B* **40** (1978) 1. doi:10.1111/j.2517-6161.1978.tb01643.x.
- [65] Osborne MA. *Bayesian Gaussian processes for sequential prediction, optimisation and quadrature*. Ph.D. thesis, Oxford University (2010).
- [66] Facebook. Ax (2019).
- [67] Balandat M, Karrer B, Jiang DR, Daulton S, Letham B, Wilson AG, et al. BoTorch: Programmable Bayesian optimization in PyTorch (2019).
- [68] Daulton S, Balandat M, Bakshy E. Differentiable expected hypervolume improvement for parallel multi-objective Bayesian optimization. *Advances in Neural Information Processing Systems* **33** (2020).
- [69] Shannon CE. A mathematical theory of communication. *Bell Labs Tech. J* **27** (1948) 379. doi:10.1002/j.1538-7305.1948.tb01338.x.
- [70] Umuroglu Y, Fraser NJ, Gambardella G, Blott M, Leong P, Jahre M, et al. FINN: A framework for fast, scalable binarized neural network inference. *Proceedings of the 2017 ACM/SIGDA International Symposium on Field-Programmable Gate Arrays* (New York, NY, USA: ACM) (2017), 65. doi:10.1145/3020078.3021744.
- [71] [Dataset] Raghu M, Gilmer J, Yosinski J, Sohl-Dickstein J. Svcca: Singular vector canonical correlation analysis for deep learning dynamics and interpretability (2017).